DOI: 10.1002/adsc.200900291

Productive Asymmetric Styrene Epoxidation Based on a Next Generation Electroenzymatic Methodology

Reto Ruinatscha,[a] Christian Dusny,[a] Katja Buehler,[a] and Andreas Schmid[a,b,*]

[a] Laboratory of Chemical Biotechnology, Department of Biochemical and Chemical Engineering, TU Dortmund University, Emil-Figge-Strasse 66, 44227 Dortmund, Germany
Fax: (+49)-231-755-7382; phone: (+49)-231-755-7380; e-mail: andreas.schmid@bci.uni-dortmund.de
[b] ISAS – Institute for Analytical Sciences, Bunsen-Kirchhoff-Strasse 11, 44139 Dortmund, Germany

Received: April 24, 2009; Revised: July 27, 2009; Published online: September 23, 2009

Abstract: We have established a novel and scalable methodology for the productive coupling of redox enzymes to reductive electrochemical cofactor regeneration relying on efficient mass transfer of the cofactor to the electron-delivering cathode. Proof of concept is provided by styrene monooxygenase (StyA) catalyzing the asymmetric (*S*)-epoxidation of styrene with high enantiomeric excess, space-time yields, and current efficiencies. Highly porous reticulated vitreous carbon electrodes, maximized in volumetric surface area, were employed in a flow-through mode to rapidly regenerate the consumed $FADH_2$ cofactor required for StyA activity. A systematic investigation of the parameters determining cofactor mass transfer revealed that low FAD concentrations and high flow rates enabled the continuous synthesis of the product (*S*)-styrene oxide at high rates, while at the same time the accumulation of the side-products acetophenone and phenylacetaldehyde was minimized. At 10 μM FAD and a flow rate of 150 mL min^{-1}, an average space-time yield of 0.35 g L^{-1} h^{-1} could be achieved during 2 h with a final (*S*)-styrene oxide yield of 75.2%. At two-fold lower aeration rates, the electroenzymatic reaction could be sustained for 12 h, albeit at the expense of lower (59%) overall space-time yields. Under these conditions, as much as 20.5% of the utilized current could be channeled into (*S*)-styrene oxide formation. In comparison with state-of-the-art electroenzymatic methodologies for the same conversion, (*S*)-styrene oxide synthesis could be improved up to 150-fold with respect to both reaction time and space-time yield. These productivities constitute the most efficient reaction reported for asymmetric *in vitro* epoxidations of styrene.

Keywords: asymmetric synthesis; cofactor regeneration; electrochemistry; enzyme catalysis; styrene monooxygenase; three-dimensional electrodes

Introduction

Asymmetric epoxidations are key transformations *en route* to biologically active pharmaceuticals and fine chemicals. The introduction of two C–O bonds in one reaction not only leads to the formation of up to two chiral centers, but also provides access to a diverse array of key intermediates due to the possibility of facile opening of the epoxide ring.[1] Much research effort has thus been dedicated to the development of efficient asymmetric epoxidations, and many practical and proficient methodologies based on transition metals have been reported[2] since the breakthroughs of Katsuki and Sharpless in the 1980s with titanium tartrate catalysts.[3] Current interests towards more economical and sustainable synthetic methodologies led to the development of less expensive, atom efficient and less toxic catalytic systems.[4,5] Such a system has recently been reported by Beller and colleagues for enantioselective epoxidations based on iron catalysts and hydrogen peroxide as oxidant.[6] In addition, chiral ketones instead of transition metals are increasingly recognized as valuable organocatalysts for asymmetric epoxidations,[7] as well as the use of molecular oxygen instead of hazardous, waste producing oxidants.[8] Although many of these future-oriented methodologies show already promising enantioselectivities, low catalyst efficiencies and low productivities often restrict their practical value.[5,7]

A potential solution for these challenges is the utilization of enzymatic epoxidation catalysts, that is, monooxygenases. Monooxygenases frequently exhibit high conversion rates at excellent enantioselectivities, are active at ambient reaction conditions, use molecular oxygen as oxidant, and are produced from natural, renewable raw materials.[9] In the case of flavin-dependent monooxygenases, the selective incorporation of one oxygen atom into the substrates, and the re-

duction of the other oxygen atom to water, is accomplished by peroxo-FAD, generated from reductive activation of molecular oxygen with $FADH_2$. As this cofactor is consumed during catalysis, it needs to be continuously supplied for the epoxidation reaction. Since $FADH_2$ is prone to rapid re-oxidation under aerobic conditions its *in situ* regeneration is essential to sustain the catalytic cycle. The most efficient enzymatic methodologies in terms of productivities employ living microbial cells as biocatalysts, performing intracellular $FADH_2$ regeneration at the expense of energy sources such as glucose,[10,11] or isolated regeneration enzymes utilizing chemical sources of reduction equivalents such as formate.[12] Alternatively, electrical power, the cheapest source of reduction equivalents for redox enzymes,[13] can be used for the reagent-free regeneration of $FADH_2$ at cathodes in cell-free epoxidations, omitting the cellular cofactor regeneration machinery and additional regeneration enzymes from the reaction.[14] In general, such electroenzymatic approaches might not only be more practical because of their simplicity, but they would also combine two environmentally friendly methods for the selective synthesis of chiral synthons.[15] Despite the potential advantages of electroenzymology, there have been some drawbacks limiting the implementation of this methodology in synthetic applications. Most of the so far developed electroenzymatic processes display insufficient reaction stabilities and too low electrochemical cofactor regeneration rates with respect to the redox enzyme used as catalyst.[16]

The driving force for high electrochemical cofactor regeneration rates is the mass transfer from the bulk solution to the depleted region near the electrode. As redox enzymes typically require very low cofactor concentrations in the micromolar to millimolar range, high cofactor amounts adjacent to electrode surfaces can only be sustained by increasing both cofactor transport rates from the bulk solution to the near-electrode volume and high volumetric electrode surface areas for increasing the volume of the near-electrode layer. By taking these considerations into account, we employed microporous, three-dimensional reticulated vitreous carbon (RVC) electrodes for improved mass transfer in a flow-through plate and frame electrochemical filter press cell, enabling high $FADH_2$ regeneration rates.[17] This system was evaluated using the $FADH_2$ dependent two-component styrene monooxygenase StyAB from *Pseudomonas* sp. VLB120 that catalyzes (*S*)-selective epoxidations of a broad range of styrene derivatives at high rates, under ambient reaction conditions with molecular oxygen as oxidant.[12,18,19] Coupling this enzyme system to the electrochemical regeneration allows us to omit the reductase component StyB from the reaction, thus simplifying the set-up.[14] We systematically evaluated this new electroenzymatic methodology for the asymmetric (*S*)-epoxidation of styrene with respect to productivities and current efficiencies.

Results

We aimed at coupling the enzymatic styrene epoxidation reaction (R1) to the electrochemical regeneration (R2) of the necessary cofactor $FADH_2$.

$$\text{styrene} + FADH_2 + O_2 \xrightarrow{StyA} \text{(S)-styrene oxide} + FAD + H_2O \quad \text{(R1)}$$

$$FAD + 2e^- + 2H^+ \xrightarrow{electrode} FADH_2 \quad \text{(R2)}$$

Space-time yields of the StyA-catalyzed styrene epoxidation reaction in the electrochemical flow-through reactor were maximized with respect to $FADH_2$ regeneration rates (STY_{FADH_2}) to meet the requirements of the flavin-dependent monooxygenase, considering:[20]

$$STY_{FADH_2} = A_V \times K_M \times c_{FAD} \quad \text{(E1)}$$

Here A_V denotes the cathode surface to volume ratio, k_M the mass transfer coefficient, and c_{FAD} the FAD concentration. The electrochemical cell was equipped with highly porous RVC electrodes having a large surface to volume ratio ($A_V = 19685\ m^2\,m^{-3}$), corresponding to nearly 1 m^2 of surface area at a cathode volume of 50 cm^3 only, while at the same time providing a high reaction volume of 45.5 cm^3. This volumetric surface area not only enabled high regeneration rates of consumed $FADH_2$ (E1), but resulted also in an optimal mass transfer due to its high porosity, serving as turbulence promoter,[21] thus shortening diffusion distances in dependence of applied flow rates.[17]

Based on these reactor characteristics, we systematically investigated the influence of flow rates (up to 50 $mL\,min^{-1}$) and FAD concentrations (up to 200 μM) at an aeration of 45 $mL\,min^{-1}$ (corresponding to 22.8 mmol molecular oxygen h^{-1}) on the average electroenzymatic space-time yield during 105 min. StyA coupled to electrochemical regeneration of $FADH_2$ catalyzed the formation of (*S*)-styrene oxide from styrene with an enantiomeric excess of 99.5%.

Average (*S*)-styrene oxide space-time yields at a flow rate of 10 $mL\,min^{-1}$ moderately increased with FAD concentrations to 0.26 $mM\,h^{-1}$. Interestingly, the electroenzymatic reaction also led to the formation of acetophenone and phenylacetaldehyde. The highest accumulation rate of these side-products (0.09 $mM\,h^{-1}$) was observed at 200 μM FAD (Figure 1 A). Up to three-fold higher space-time

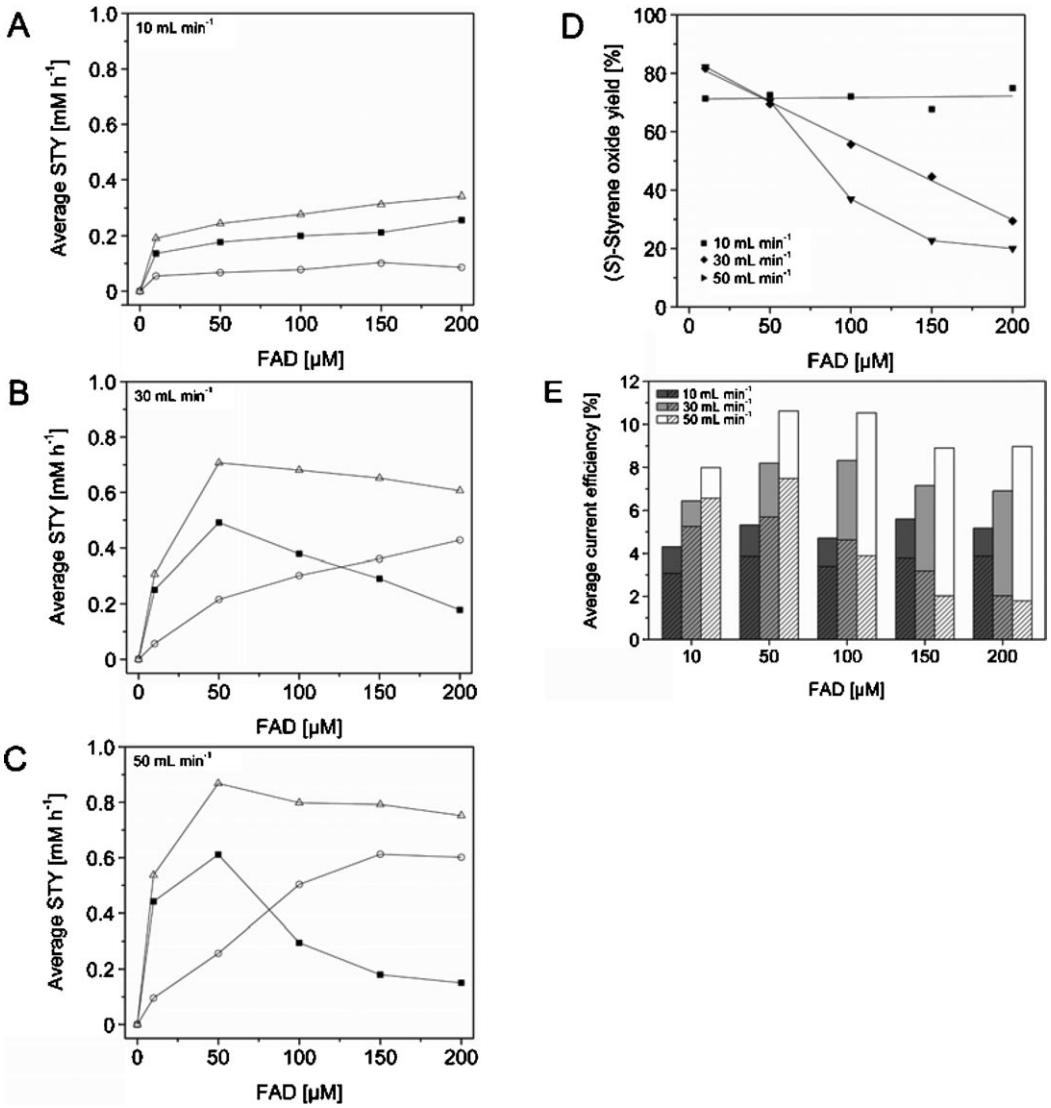

Figure 1. Electroenzymatic reaction performances as a function of FAD concentration and flow rate during 105 min. (**A–C**) Average space-time yields (STY) for (*S*)-styrene oxide (■), acetophenone and phenylacetaldehyde (○), and total products formed (△). (**D**) Corresponding (*S*)-styrene oxide yields over the totally formed products. (**E**) Average current efficiencies for (*S*)-styrene oxide (shaded bars) and the side-products (unshaded bars).

yields regarding overall product formation were observed at a flow rate of 30 mL min^{-1}. However, under this condition average (*S*)-styrene oxide space-time yields were maximal at already 50 μM FAD (0.49 mM h^{-1}), while acetophenone and phenylacetaldehyde space-time yields still increased in conjunction with the FAD concentrations, finally accounting for 70.6% of the totally formed products at 200 μM FAD (Figure 1B). Increasing the flow rate to 50 mL min^{-1} not only further enhanced overall electroenzymatic space-time yields, but also led to a more distinctive (*S*)-styrene oxide space-time yield maximum at 50 μM FAD (0.61 mM h^{-1}) (Figure 1C).

Overall, side-product formation rates were strongly dependent on both increasing FAD concentrations and flow rates above 10 mL min^{-1}. Accordingly, up to 82.2% (*S*)-styrene oxide yields were achieved at 10 μM FAD and 10 mL min^{-1} (Figure 1D). Highest current efficiencies (100% efficiency corresponds to the utilization of 2 electrons per molecule of product, based on the reaction stoichiometry) were generally observed between 50 μM and 100 μM FAD. Average current efficiencies with respect to all products formed were mainly determined by the flow rates, and were in the range of 5.0% ± 0.5% at 10 mL min^{-1}, 7.5% ± 0.8% at 30 mL min^{-1}, and 9.4% ± 1.0% at 50 mL min^{-1}. In contrast, average (*S*)-styrene oxide current efficiencies were strongly affected by FAD concentrations and flow rates above 10 mL min^{-1}. Highest current utilization (7.5%) for the epoxidation reaction was observed at 50 mL min^{-1} and 50 μM FAD (Figure 1E).

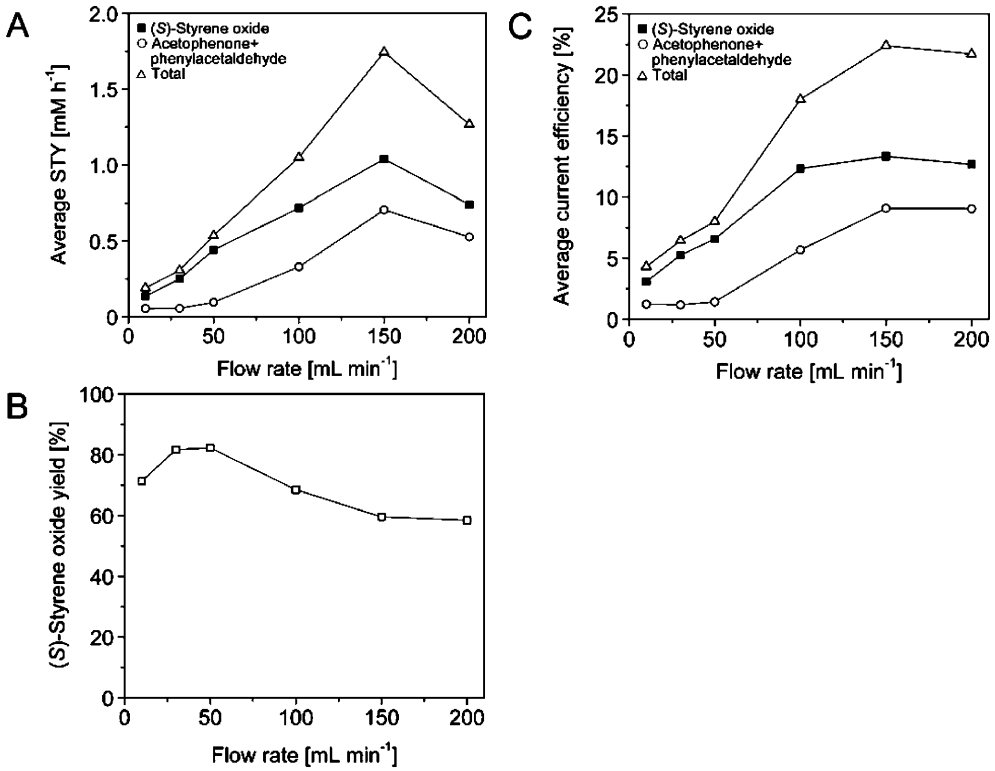

Figure 2. (**A**) Average electroenzymatic space-time yields (STY) at flow rates from 10 mL min^{-1} to 200 mL min^{-1} (10 μM FAD) during 105 min. (**B**) Corresponding (*S*)-styrene oxide yields over the totally formed products. (**C**) Average current efficiencies for (*S*)-styrene oxide, the side-products acetophenone and phenylacetaldehyde, and the totally formed products.

The performance of the electroenzymatic system was investigated in more detail at 10 μM FAD since highest (*S*)-styrene oxide yields were achieved at this cofactor concentration. Increasing the flow rates to 200 mL min^{-1} had a significant impact on space-time yields, (*S*)-styrene oxide yields, and current efficiencies. The maximum (*S*)-styrene oxide yields were determined at 50 mL min^{-1} (82.2%) (Figure 2B). The overall productivity was highest at 150 mL min^{-1} (1.7 mM h^{-1}) (Figure 2A), indicating that the enzyme stability was significantly impaired at elevated flow rates. Average current efficiencies reached a maximum at 150 mL min^{-1} of 13.3% for (*S*)-styrene oxide and 22.4% with respect to the totally formed products (Figure 2C). Apparently the transfer efficiency of electrochemically reduced FAD to StyA could not further be improved above flow rates of 150 mL min^{-1}.

During all electroenzymatic synthesis, white foam accumulated at the aqueous/organic interphase of the cathodic styrene feed/product extraction reservoir in the course of aeration. According to SDS-PAGE analysis (Figure 3A), this precipitate accumulation could be attributed to StyA and catalase denaturation in the catholyte, resulting in nearly complete termination of product formation after 120 min. Supplementation of the catholyte with either antifoam 204 for foam avoidance or with a mixture of antifoam 204, BSA and sucrose resulted in a constant (*S*)-styrene oxide formation rate over at least 120 min (10 μM FAD, 150 mL min^{-1}) and a significantly lowered enzyme precipitation (Figure 3A). In comparison to the non-stabilized reaction system, addition of antifoam 204 resulted in 34% lower initial (*S*)-styrene oxide formation rates, whereas additional supplementation with BSA and sucrose could sustain the initial styrene epoxidation rate (Figure 3B). Current efficiencies with respect to (*S*)-styrene oxide were around 12% for the non-stabilized and the antifoam 204 supplemented electroenzymatic reaction system. A 40% higher current efficiency was determined for the reaction system containing all three stabilizers. Apparently the efficient utilization of electrochemically generated $FADH_2$ correlates with the amount of active StyA.

The electroenzymatic reaction system stabilized with antifoam 204, BSA, and sucrose was evaluated for maximal productivities at 10 μM FAD and 150 mL min^{-1} regarding synthesis times and aeration rates. At the initially applied aeration with 22.8 mmol h^{-1} molecular oxygen, up to 6.9 mM (*S*)-styrene oxide could be synthesized within 12 h, which was equivalent to an average space-time yield of 0.1 g L^{-1} h^{-1} (Synthesis 1, Table 1). Under these conditions, the average current efficiency was 20.5%. Con-

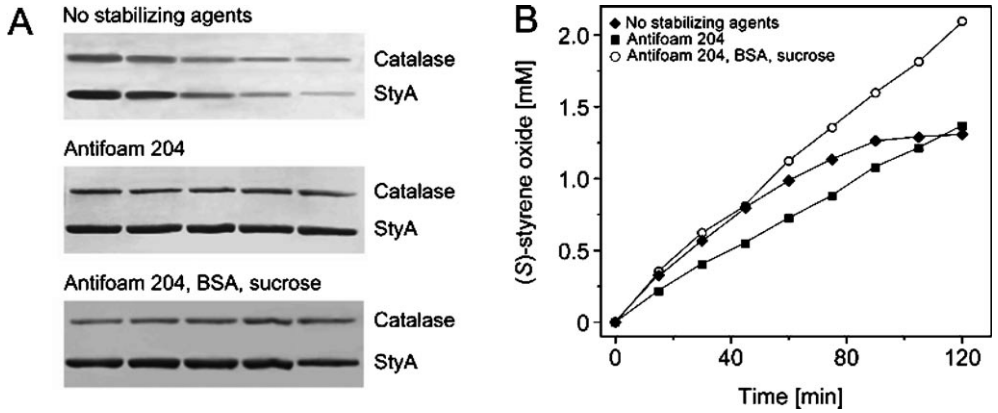

Figure 3. (**A**) Influence of stabilizing agents in the cathodic storage reservoir on StyA and catalase precipitation at the aqueous/organic interphase, visualized by SDS-PAGE. (**B**) Influence of the stabilizing agents on (*S*)-styrene oxide formation rates. Experimental conditions: 10 μM FAD, 150 mL min^{-1}.

sidering the concurrent side-product formation, the average overall electroenzymatic space-time yield was 0.15 g L^{-1} h^{-1} with a current utilization efficiency of 30.7%. Instead of forming white precipitates at the aqueous/organic interphase of the cathodic reservoir, the stabilized reaction mixture became slightly turbid over time. This observation was much more pronounced at the higher aeration rate, pointing to enzyme denaturation by shear stress (Synthesis 2, Table 1). Changing the aeration mode from a capillary to an HPLC frit for finer dispersion and distribution of the supplied air, while at the same time increasing the molecular oxygen input to 46.8 mmol h^{-1}, more than doubled average (*S*)-styrene oxide and overall space-time yields to 0.26 g L^{-1} h^{-1} and 0.35 g L^{-1} h^{-1}, respectively. However, product formation stopped after 120 min, thereby leading to a final (*S*)-styrene oxide concentration of 3.5 mM (Figure 4). Average current efficiencies were almost four times lower than at the lower aeration rate, presumably due to increased cathodic reduction of molecular oxygen to hydrogen peroxide. Electroenzymatic syntheses performances are summarized in Table 1.

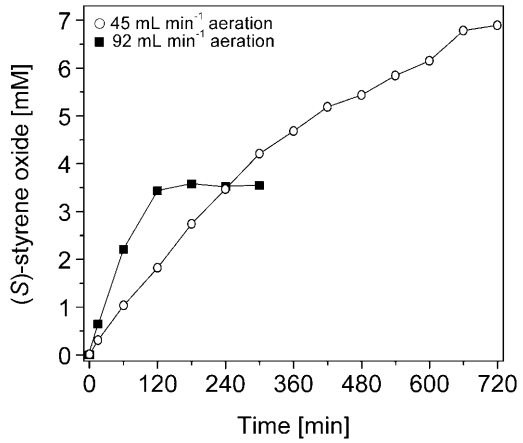

Figure 4. Electroenzymatic syntheses of (*S*)-styrene oxide at a molecular oxygen input of 45 mL min^{-1} (Synthesis 1) and 92 mL min^{-1} (Synthesis 2), stabilized with a mixture of antifoam 204, BSA, and sucrose. Flow rate: 150 mL min^{-1}, FAD: 10 μM.

Table 1. Overall electroenzymatic synthesis performance at a molecular oxygen input of 22.8 mmol h^{-1} (45 mL min^{-1} air) and 46.8 mmol h^{-1} (92 mL min^{-1} air), stabilized with a mixture of antifoam 204, BSA, and sucrose. Flow rate: 150 mL min^{-1}, FAD: 10 μM.

	Synthesis 1		Synthesis 2	
Parameter	(*S*)-styrene oxide	Total[a]	(*S*)-styrene oxide	Total[a]
STY,[b] mM h^{-1} (g L^{-1} h^{-1})	0.8 (0.10)	1.2 (0.14)	2.2 (0.26)	2.9 (0.35)
Current efficiency,[b] %	20.5	30.7	5.7	7.4
Final concentration, mM (g L^{-1})	6.9 (0.83)	10.5 (1.26)	3.5 (0.42)	4.6 (0.55)
Aeration, mL min^{-1} (mmol O_2 h^{-1})	45 (22.8)		92 (46.8)	
Duration, h	12		2	

[a] Including acetophenone and phenylacetaldehyde.
[b] Average value during synthesis.

Discussion

The simultaneous maximization of volumetric electrode surface areas (A_V) and mass transfer coefficients (k_M) is a common practice in electrochemical engineering to optimize electrochemical process performances with respect to space-time yields (E1). Based on these considerations, we employed highly porous and volumetric surface area maximized RVC electrodes to accelerate volumetric $FADH_2$ regeneration rates, as they are stoichiometrically coupled to StyA space-time yields (R2+R1). Since mass transfer can be influenced by the flow rates through the porous foam electrodes and the concentration of the cofactor, the influence of both parameters on electroenzymatic space-time yields was systematically evaluated.

At a constant FAD concentration, space-time yields and current efficiencies steadily increased up to a flow rate of 150 mL min^{-1}. Above this flow rate electroenzymatic space-time yields decreased, indicating StyA denaturation (Figure 2). We assume that the porous structure of the electrode may cause high shear stress. Moreover, the foam formation observed in the cathodic storage reservoir independent of the flow rate points to additional shear stress due to the aeration of the system. The loss of active enzyme could be minimized by the addition of a mixture of antifoam 204, BSA, and sucrose, all well known protein stabilizers.[12,22] Inactivation of StyA by hydrogen peroxide, generated in the course of $FADH_2$ uncoupling (R3–R5), was counteracted using catalase. As $FADH_2$ uncoupling reactions also generate superoxide, addition of superoxide dismutase could be beneficial to increase the stability of StyA, and hence the productivity of the electroenzymatic reaction.

Increasing FAD concentrations negatively influenced (*S*)-styrene oxide space-time yields and (*S*)-styrene oxide current efficiencies due to the enhanced accumulation of the side-products acetophenone and phenylacetaldehyde (Figure 1). These observations may be attributed to the chemical behaviour of FAD and $FADH_2$ in solution. Whereas $FADH_2$ is continuously regenerated at the cathodes, the reduced $FADH^-$ anion, which is in equilibrium with $FADH_2$ ($pK_a \sim 6.5$)[23], and FAD symproportionate nearly diffusion-controlled to semiquinone radicals (R3) that are rapidly re-oxidized to FAD by one-electron acceptors such as molecular oxygen (R4). The transiently formed superoxide finally leads to the accumulation of hydrogen peroxide (R5):[24]

As a result of the nearly diffusion controlled chemical uncoupling reactions, a reactive near-cathode layer consisting of FAD, $FADH_2$, semiquinone radicals, and superoxide formed during electrochemical FAD reduction, while hydrogen peroxide accumulation was minimized due to the presence of catalase. $FADH_2$ was therefore only available for StyA catalysis in close proximity to the cathode surfaces at a certain steady state concentration, determining electroenzymatic space-time yields. Since the accumulation of the side-products acetophenone and phenylacetaldehyde was dependent on StyA activity (Figure 1 A–C, Figure 2 A), and hence on local (*S*)-styrene oxide concentrations within the reactive near-cathode region, it is very likely that the observed side-products originated from radicalic semiquinone attack of *in situ* generated (*S*)-styrene oxide (Figure 5). Similar rearrangements of epoxides to the corresponding carbonyl compounds in presence of radicals are described in literature.[25]

Accordingly, we observed at improved FAD mass transfer conditions (raising flow rates, elevated FAD concentrations), and hence faster semiquinone formation rates, an increasing accumulation of these side-products at the expense of (*S*)-styrene oxide (Figure 1 D), as well as lowered (*S*)-styrene oxide current efficiencies (Figure 1 E). Based on these observations we assume that the theoretical electroenzymatic reaction performance is reflected by the overall space-time yields including side-products. Overall space-time yields slightly decreased at FAD concentrations above 50 μM, suggesting that the steady state $FADH_2$ concentration within the reactive near-cathode layer was also lowered. Apparently, under these conditions, reduced FAD was increasingly channelled into uncoupling reactions (R3–R5) than the enzymatic product

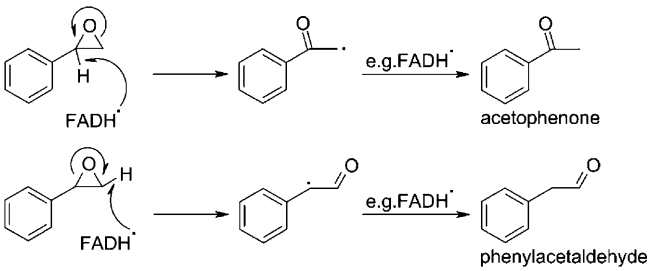

Figure 5. Proposed reaction scheme for the side-products (acetophenone and phenylacetaldehyde) formed during electroenzymatic styrene oxide synthesis.

$$FADH^- + FAD + H^+ \underset{k_{-1}}{\overset{k_1}{\rightleftharpoons}} 2\,FADH^\bullet \quad (k_1 \sim 10^6\ M^{-1}\,s^{-1},\ k_{-1} \sim 5 \times 10^8\ M^{-1}\,s^{-1}) \qquad (R3)$$

$$FADH^\bullet + O_2 \xrightarrow{k_2} 2\,FAD + O_2^- + H^+ \quad (k_2 \sim 10^4\ M^{-1}\,s^{-1} \text{ to } 10^8\ M^{-1}\,s^{-1}) \qquad (R4)$$

$$FADH^\bullet + O_2^- + H^+ \xrightarrow{k_3} FAD + H_2O_2 \quad (k_3 \sim 10^8\ M^{-1}\,s^{-1}) \qquad (R5)$$

formation (R1). This FAD concentration-dependent re-oxidation may also explain why elevated flow rates at constant FAD concentrations could steadily increase overall space-time yields (Figure 2 A).

In a related study we have evaluated the influence of initial FAD concentration on FAD reduction rates for the electrochemical sub-reaction using the same electrochemical cofactor regeneration module.[17] Anaerobic conditions were applied to minimize uncoupling reactions of reduced FAD with molecular oxygen, and thus to determine the maximal FAD reduction rates possible with this system. In contrast to the electroenzymatic reaction system described here, where FAD concentrations higher than 50 μM did not further improve productivities, electrochemical reduction rates steadily increased up to 360 mM FAD to 93 $mM\,h^{-1}$. Comparison of the two reaction systems under similar reaction conditions (e.g., 50 μM FAD, 30 $mL\,min^{-1}$ flow rate) indicates that electroenzymatic (*S*)-styrene oxide space-time yields are by a factor of 60 lower than the possible electrochemical FAD reduction rate. Several aspects have to be taken into account when comparing this seemingly huge difference. Firstly, at 50 μM FAD and a flow rate of 30 $mL\,min^{-1}$, only 4% of the consumed current was channeled *via* $FADH_2$ into (*S*)-styrene oxide formation. Since $FADH_2$ rapidly uncouples to the enzymatically inactive FAD cofactor (R3–R5) prior to reaching StyA, it can be assumed that the net concentration of reduced FAD available for the enzymatic conversion was much lower than the initial 50 μM. As electrochemical reduction rates were shown to increase with the applied FAD concentration, electrochemical FAD reduction rates can only be compared with the electroenzymatic productivities on the basis of identical initial and net cofactor concentrations, respectively. Secondly, according to Michaelis–Menten, enzymatic productivities are a function of enzyme concentration. Application of a higher StyA concentration might therefore be useful to channel more of the reduced FAD cofactor into the epoxidation reaction (R1) than in non-productive uncoupling reactions (R3–R5), and to overcome enzymatic reaction rate limitations. For instance, in the previously mentioned study using the same electrochemical cofactor regeneration module,[17] StyA was added to the reaction to demonstrate electroenzymatic coupling. Application of a 2.5 times higher StyA concentration than in the electroenzymatic reactions described here resulted in correspondingly higher (*S*)-styrene oxide space-time yields. Furthermore, in case of the electroenzymatic process using StyA, productivities were strongly depending on the molecular oxygen input. Increasing the aeration by a factor of two more than doubled (*S*)-styrene oxide and overall space-time yields (Figure 4, Table 1), which points to substrate limitation by molecular oxygen. Therefore, enzymatic sub-reactions need to be optimized in order to achieve electroenzymatic productivities close to the possible electrochemical cofactor regeneration rate.

State-of-the-art electrochemical regeneration systems for the reductive regeneration of cofactors commonly employ cylindrical electrodes in batch cells.[16,26] Since mixing needs to be carried out by a stirrer, these reactor systems are generally characterized by low electrode surface areas per reaction volume, as well as impaired mass transport from the stirred bulk solution to distant electrode surfaces. Volumetric cofactor regeneration rates are thus very likely to be limiting the enzymatic synthesis reaction. In contrast, the presented electrochemical reactor design enables high volumetric regeneration rates of $FADH_2$ in close proximity to StyA due to the employed three-dimensional microporous cathodes providing high cofactor mass transfer. This is of utmost importance in the case of oxygen-dependent redox enzymes. These enzymes are dependent on molecular oxygen as a co-substrate, and their reduced cofactors (e.g., flavins) or mediators (commonly cobalt sepulchrate, or methyl viologens)[26,27] are often capable of performing radicalic one-electron chemistry. Since molecular oxygen naturally exists as a diradical in its ground state, fast uncoupling reactions with reduced cofactors and/or mediators are always very likely to occur.[24,28,29] These uncoupling reactions not only impair the net cofactor regeneration rates, but they may also limit the concentration of enzymatically active cofactors. As a result, space-time yields of cofactor mass transfer non-optimized systems are usually rather low with respect to the maximal activity of the production enzyme[16] because of fast competing side-reactions. For example, cytochrome P450cam coupled to the reductive electrochemical regeneration of putidaredoxin exhibited around 3% of the native activity with respect to 5-*exo*-hydroxy camphor formation from camphor,[30] cytochrom P450 BM3 regenerated by 1,10-dicarboxycobaltocene was able to hydroxylate lauric acid up to 3.6% of the theoretical rate,[29,31] and StyA coupled to the reductive electrochemical regeneration of $FADH_2$ exhibited only 0.6% of the native (*S*)-epoxidation activity towards styrene.[14]

In comparison to the previously described electroenzymatic batch reaction system employing StyA,[14] we were able to exploit up to 8.7% of the native initial enzyme activity (2.1 $U\,mg^{-1}$)[19] with respect to (*S*)-styrene oxide space-time yields, and up to 11.5% regarding overall space-time yields (Synthesis 2). Furthermore, the presented electroenzymatic approach did not only permit higher enzyme activities than the corresponding batch approach,[14] but also allowed for longer synthesis times. Moreover, productivity in terms specific enzyme activity and synthesis time was 150-fold higher regarding (*S*)-styrene oxide, and 215-

fold higher with respect to the overall electroenzymatic performance. In comparisons of electroenzymatic and native activities it has to be noted that in the natural system, StyA activities are dependent on the FAD reductase component StyB,[19] which is not required in electroenzymatic reactions using StyA. StyA and StyB are assumed to form transient, equimolar complexes during catalysis,[32] possibly altering catalytic properties of StyA, thereby making a direct comparison of native and electroenzymatic StyA activities difficult. Surprisingly however, when comparing electroenzymatic StyA activities achieved in this study with native StyA activity under process conditions, the electroenzymatic approach was at least 40% more productive with respect to the average specific enzyme productivity.[12]

Cellular and enzymatic cofactor regeneration methodologies are generally stated to be the most efficient and productive for the application of redox enzymes.[33] However, whereas for whole cell styrene epoxidation an average specific (*S*)-styrene oxide production rate of 2.6 g g_{StyA}^{-1} h^{-1} during 10 h at an electron efficiency of 10% is reported,[10,34] the here presented electroenzymatic methodology could channel more than 20% of the consumed electrons into (*S*)-styrene oxide for at least 12 h at an average specific (*S*)-styrene oxide production rate of 0.5 g g_{StyA}^{-1} h^{-1} (Table 2). This exceeds the corresponding *in vitro* enzymatic $FADH_2$ regeneration approach, where an average specific styrene oxide production rate of 0.35 g g_{StyA}^{-1} h^{-1} (based on the epoxidation activity towards 3-chlorostyrene) was reached during 10.5 h.[12] However, a drawback of the developed electroenzymatic styrene epoxidation constitutes the side-product formation, which was under synthesis conditions (Synthesis 1) up to 2.5 times higher than for the corresponding whole-cell process (13%).[35] Interestingly, for this whole-cell process only the formation of 2-phenylethanol was reported, whereas neither acetophenone nor phenylacetaldehyde could be observed.

Conclusions

The present study shows that isolated monooxygenases can efficiently and productively be coupled to reductive electrochemical cofactor regeneration for the synthesis of high value products. With this engineering approach it could be demonstrated that even a fast re-oxidizing $FADH_2$ cofactor can be regenerated at high overall rates, allowing for the productive coupling of styrene monooxygenase (StyA) for the synthesis of (*S*)-styrene oxide. Next to the achieved synthesis performances, which are already in the same range as for whole-cell methodologies, the employed electrochemical flow reactor design might also be suitable for scale-up, as has been demonstrated in industrial electro organic processes.[20] We therefore expect that further developments of electroenzymatic methodologies relying on mass transfer improved regeneration of diffusible cofactors/mediators may help establishing sustainable redox enzyme catalysis (e.g., using flavin-fusion enzymes like cytochrome P450 BM-3 monooxygenases) beyond lab-scale.

Experimental Section

Materials

Nitrogen 5.0 was supplied by Air-Liquide (Düsseldorf, Germany). Chemicals, catalase, and bovine serum albumin were purchased from Sigma–Aldrich (Steinheim, Germany) in the highest quality available and were used without further purification. Buffers were prepared according to Beynon and Easterby[36] using ultra-pure water from a Seralpur PRO 90 CN system (Seral, Germany). Solvents were obtained from Fischer Scientific GmbH (Schwerte, Germany). For protein quantification according to Bradford,[37] the Quick Start kit from Bio-Rad Laboratories GmbH (Munich, Germany) was used with bovine serum albumin as standard.

Table 2. Comparison of different reaction concepts for the biocatalytic synthesis of (*S*)-styrene oxide utilizing StyA as biocatalyst.

Reaction concept	Specific (*S*)-styrene oxide formation rate [g g_{StyA} h^{-1}]	STY [mM h^{-1}]	Total running time [h]	Electron efficiency [%]	Ref.
Whole cell	2.6[a]	30.6	10	10[b]	[10, 34]
Natural system *in vitro*[c]	0.35	6.2	10.5	n.d.	[12]
Electroenzymatic concept	0.5[d], 1.3[e]	0.8[d], 2.2[e]	12[d], 2[e]	20.5[d], 5.7[e]	this study

[a] Assuming that proteins account for 50% of dry cell mass, and StyA overexpression is 25%.[19]
[b] Based on glucose as electron source.
[c] Based on the epoxidation activity towards 3-chlorostyrene.
[d] Synthesis 1.
[e] Synthesis 2.

Production of Styrene Monooxygenase Component StyA

The *styA* gene was overexpressed in *E. coli* JM101 (pSPZ10) and purified as described in the literature.[19] The purification method was modified as follows: clarified supernatants were loaded onto an XK16/20 column (Amersham Biosciences, Dübendorf, Switzerland) filled with 28 mL of Sepabeads EB-QA405 at a flow rate of 2 mL min^{-1} in 20 mM Tris pH 6.8. Elution was performed at the same flow rate by applying a linear gradient of 2 mM NaCl min^{-1} in 20 mM Tris pH 6.8. StyA was fractionated from 40 mM to 240 mM NaCl. During hydrophobic interaction chromatography, elution of StyA was achieved by applying a linear gradient from 1.6 M to 0.8 M $(NH_4)_2SO_4$ using 20 mM Tris pH 7.15, at a rate of 11.8 mM min^{-1}. Fractions were collected from 1.4 M to 1.1 M $(NH_4)_2SO_4$. Desalting was carried out using Sephadex G25 medium packed in a 16/20 column (Amersham Biosciences, Dübendorf, Switzerland) at a flow rate of 5 mL min^{-1} in 200 mM potassium phosphate buffer pH 7.25 (buffer that was used later for electroenzymatic syntheses). Fractions were concentrated 200-fold using 30.0 kDA MWCO Amicon Ultra-15 Centrifugal Filters (Millipore Corporation, Schwalbach, Germany) at 3990 × *g* (4 °C), aliquoted to a concentration of 5 mg mL^{-1} and stored at −20 °C. StyA stocks were stored no longer than two weeks prior to use.

Electrochemical Cell

The electrochemical cell was developed for continuous electroenzymatic syntheses and was constructed as a lab-scale plate and frame filter press cell.[38] Anodes and cathodes consisted of three-dimensional reticulated vitreous carbon (RVC) flow-through electrodes (ERG Materials and Aerospace Corporation, Oakland, CA) having a pore grade of 100 nominal pores per inch (ppi) and being threefold compressed (Figure 6 A). Both electrodes (1 cm × 5 cm × 10 cm) were moulded into poly(tetrafluoroethene) (PTFE) frame units (0.8 cm × 5 cm × 10 cm) and were separated by a Nafion N324 membrane (DuPont de Nemours, Bad Homburg, Germany). Leak-proof construction was ensured by placing silicon gaskets on both frame sides. Cover plates were made out of glass. The cell assembly was compressed by means of screw-couplings. External electrical contacting was accomplished by screwable, PTFE sealed platinum plugs. An RE-5B Ag|AgCl reference electrode (Bioanalytical Systems Inc., Warwickshir, UK) complemented the three-electrode set-up. Electrolyte circulation was maintained in longitudinal direction, vertically upwards, by means of triple distribution devices placed on both sides for efficient electrode flow-through. Separate anolyte and catholyte circulation was carried out with PrepStar SD-1 Solvent Delivery Modules (Varian Deutschland GmbH, Darmstadt, Germany), connected to the electrolysis cell and the anodic or cathodic storage reservoirs by means of PTFE tubings (CS-Chromatographie GmbH, Langerwehe, Germany) and VITON Fluran HCA F-5500 A (ISMATEC GmbH, Wertheim-Mondfeld, Germany) connectors.

Electrochemical Maintenance Procedures

Nafion N324 membranes were cleaned four times sequentially with 3% H_2O_2, 1 N H_2SO_4, and water (80 °C, 1 h) prior to first use.[39] RVC electrodes were treated with ultrasound in methanol, water, and 200 mM potassium phosphate buffer pH 7.25 (30 min each) before first use. Regular electrochemical electrode conditioning was carried out in 200 mM potassium phosphate buffer (pH 7.25, 30 °C) by applying cycling potentials between −0.9 V and +0.9 V versus Ag/AgCl for 3 min and 5 times each,[40] at a flow-rate of 15 mL min^{-1} (room temperature).

Electroenzymatic Syntheses

Anolyte (200 mL) and catholyte (120 mL) solutions consisted both of 200 mM potassium phosphate buffer pH 7.25 (30 °C). Throughout the experiments, anodic and cathodic

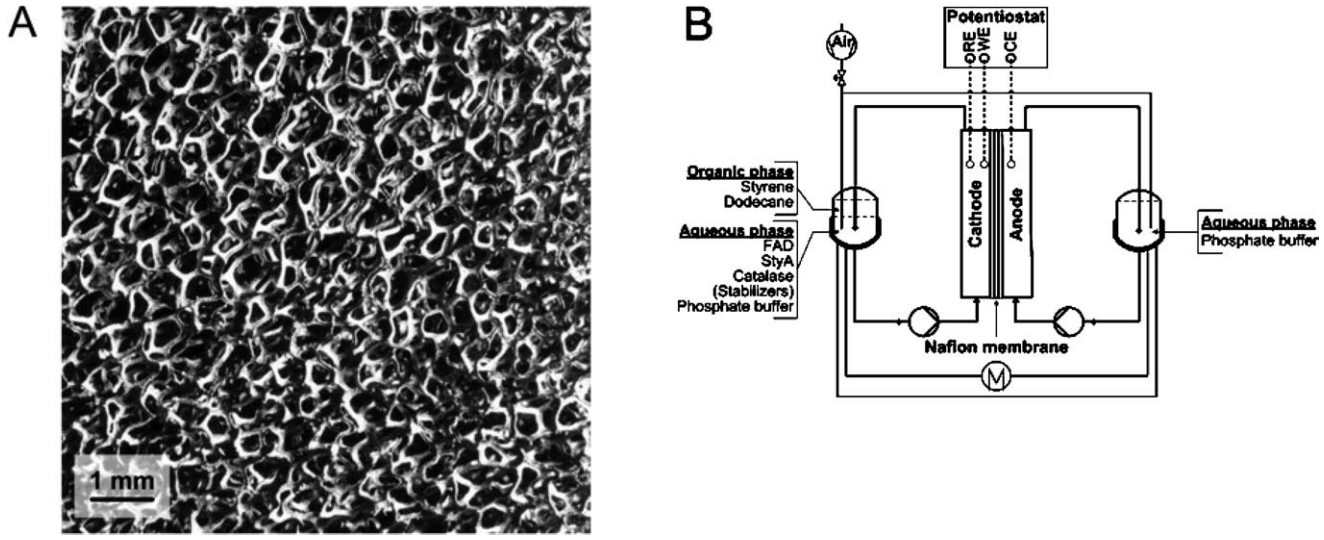

Figure 6. (**A**) Micrograph of the employed three-fold compressed 100 ppi reticulated vitreous carbon (RVC) electrodes (adapted from http://www.ergaerospace.com). (**B**) Electroenzymatic reaction set-up. ADC: Analog-to-digital converter channel, CE: counter electrode (anode), RE: reference electrode, WE: working electrode (cathode).

storage reservoirs were kept at 37 °C in order to maintain constant electrolyte temperatures of 30 °C inside the electrochemical reactor. Before each synthesis reaction, FAD ($\varepsilon_{450nm} = 11.3\ mM^{-1}cm^{-1}$)[41] was added to the catholyte and concentrations were adjusted using a Libra S11 photometer (Biochrom LTD, Cambridge, UK) at equilibration, and under continuous pumping ($30\ mL\,min^{-1}$). Subsequently, StyA was added to a final catholyte concentration of $0.2\ mg\,mL^{-1}$, as well as 2000 U mL^{-1} catalase. Enzyme stabilizing agents were added optionally to the catholyte in the following aqueous concentrations: $0.5\ \mu L\,mL^{-1}$ antifoam 204, $2.5\ mg\,mL^{-1}$ BSA (bovine serum albumin), and $20\ mg\,mL^{-1}$ sucrose. Pre-equilibration of the reaction system was done as follows: anolyte and catholyte were both circulated for 10 min at $30\ mL\,min^{-1}$. Afterwards, the catholyte was covered with 50 mL dodecane and 6.5 mL styrene (1 M), following electrolyte circulation for another 30 min at the same flow rate. Subsequently, defined reaction conditions were applied by adjusting flow-rates ($10\ mL\,min^{-1}$ to $200\ mL^{-1}$) and aeration (45 mL air min^{-1} by means of a capillary, or 92 mL air min^{-1} using an HPLC frit) into the cathodic storage reservoir. Syntheses were started 3 min later by applying a cathodic potential of −0.75 V versus Ag|AgCl. Reaction control and data recording was performed with an Autolab PGSTAT 302 instrument unit (Deutsche Metrohm GmbH & Co. KG, Filderstadt, Germany), equipped with General Purpose Electrochemical System (GPES) software (version 4.9.006 for Windows) (Figure 6B).

Sample Preparation and Analysis

Aqueous phase samples were diluted with an equal volume of ice cold acetonitrile. Organic phase samples were extracted with an equal volume of water. Both samples were mixed in a vertically positioned Eppendorf thermo mixer (Eppendorf, Hamburg, Germany) for 2 min (1400 rpm, 10 °C), followed by centrifugation for 5 min (4 °C, $16200 \times g$) in a Heraeus Fresco 17 Microcentrifuge (Thermo Electron Corporation, Langenselbold, Germany). Aqueous phases of the organic samples were directly analyzed by reversed phase HPLC. In contrast, samples diluted in acetonitrile were mixed by gentle inversion prior to reversed phase HPLC analysis. Concentrations of styrene, (*S*)-styrene oxide, and the side-products acetophenone and phenylacetaldehyde were determined by HPLC on a LaChrom Elite Merck-Hitachi system (Darmstadt, Germany) equipped with a diode array detector and a reverse phase CC Nucleosil 100–5 C18 HD (Machery-Nagel, Oensingen, Switzerland) column. Injected sample volumes were 60 µL, mobile phase consisted of water and acetonitrile (ratio 60:40), elution was isocratic ($1\ mL\,min^{-1}$), and isotherm (25 °C). The substances were identified by comparing the retention times to commercially available standards. Quantifications were carried out by means of standard curves, recorded under identical conditions as aqueous phase samples, and organic phase samples, respectively. Space-time yields were normalized to the cathode void volume of the electrochemical cell (45.5 mL), in order to determine catalyst productivities per reaction volume. Unless indicated otherwise, average space-time yields were calculated based on the space-time yields obtained from regular sampling intervals of 15 min.

For determination of enantiomeric excesses (*ee*), reaction mixtures were extracted with diethyl ether and dried over Na_2SO_4 prior to analysis. Enantiomeric excesses were calculated using the equation $ee = |(S-R)|/(S+R)$, with *S* and *R* representing the concentrations of the two stereoisomers. Analysis was performed by gas chromatography on a Finnigan Focus GC (Thermo Electron Corporation, Langenselbold, Germany) equipped with a FI detector and a RT-BetaDEXsm ($0.25\ mm \times 0.25\ \mu m \times 30\ m$, Restek GmbH, Bad Homburg, Germany) column, using a temperature ramp from 60 °C to 100 °C (1 °C min^{-1}) with nitrogen as carrier gas.

Acknowledgements

The authors express their gratitude to Dr. Klaus-Michael Mangold (Karl-Winnacker-Institut der DECHEMA e.V., Frankfurt) and Prof. Dr. Ing. Jakob Jörissen (Department of Biochemical and Chemical Engineering, TU Dortmund) for helpful discussions and their support in designing the electrochemical cell. Furthermore, we thank Mr. Klaus Hirschfeld and Mr. Peter Schmitz (Department of Biochemical and Chemical Engineering, TU Dortmund) for expert fabrication of the electrochemical cell, and D. Ream (ERG Materials and Aerospace Corporation, Oakland, CA) for excellent technical advice. This work was financially supported by the Deutsche Bundesstiftung Umwelt (ICBio, AZ 13123-32), by the Zentrum für Angewandte Chemische Genomik, the European Union (EFRE) and by the Ministry of Innovation, Science, Research and Technology of North Rhine-Westphalia.

References

[1] a) E. N. Jacobsen, A. Pfaltz, H. Yamamoto, (Eds.), *Comprehensive Asymmetric Catalysis*, Springer, Berlin, **2004**; b) U. Sundermeier, C. Döbler, M. Beller, *Modern Oxidation Methods*, Wiley-VCH, Weinheim, **2004**; c) M. Christmann, S. Bräse, *Asymmetric Synthesis: The Essentials*, 2nd edn., Wiley-VCH, Weinheim, **2007**.

[2] a) W. Zhang, J. L. Loebach, S. R. Wilson, E. N. Jacobsen, *J. Am. Chem. Soc.* **1990**, *112*, 2801–2803; b) A. U. Barlan, A. Basak, H. Yamamoto, *Angew. Chem.* **2006**, *118*, 5981–5984; *Angew. Chem. Int. Ed.* **2006**, *45*, 5849–5852; c) W. Zhang, H. Yamamoto, *J. Am. Chem. Soc.* **2007**, *129*, 286–287.

[3] T. Katsuki, K. B. Sharpless, *J. Am. Chem. Soc.* **1980**, *102*, 5974–5976.

[4] D. Lenoir, *Angew. Chem.* **2006**, *118*, 3280–3284; *Angew. Chem. Int. Ed.* **2006**, *45*, 3206–3210.

[5] S. Enthaler, K. Junge, M. Beller, *Angew. Chem.* **2008**, *120*, 3363–3367; *Angew. Chem. Int. Ed.* **2008**, *47*, 3317–3321.

[6] F. G. Gelalcha, B. Bitterlich, G. Anilkumar, M. K. Tse, M. Beller, *Angew. Chem.* **2007**, *119*, 7431–7435; *Angew. Chem. Int. Ed.* **2007**, *46*, 7293–7296.

[7] Y. Shi, *Acc. Chem. Res.* **2004**, *37*, 488–496.

[8] C. J. Chang, J. A. Labinger, H. B. Gray, *Inorg. Chem.* **1997**, *36*, 5927–5930.

[9] W. J. H. van Berkel, N. M. Kamerbeek, M. W. Fraaije, *J. Biotechnol.* **2006**, *124*, 670–689.

[10] J.-B. Park, B. Bühler, T. Habicher, B. Hauer, S. Panke, B. Witholt, A. Schmid, *Biotechnol. Bioeng.* **2006**, *95*, 501–512.
[11] R. Gross, B. Hauer, K. Otto, A. Schmid, *Biotechnol. Bioeng.* **2007**, *98*, 1123–1134.
[12] K. Hofstetter, J. Lutz, I. Lang, B. Witholt, A. Schmid, *Angew. Chem.* **2004**, *116*, 2215–2218; *Angew. Chem. Int. Ed.* **2004**, *43*, 2163–2166.
[13] C. Wandrey, *Chem. Rec.* **2004**, *4*, 254–265.
[14] F. Hollmann, K. Hofstetter, T. Habicher, B. Hauer, A. Schmid, *J. Am. Chem. Soc.* **2005**, *127*, 6540–6541.
[15] E. Steckhan, *Topics in Current Chemistry*, Vol. 170, Springer, Berlin, **1994**.
[16] R. Ruinatscha, V. Höllrigl, K. Otto, A. Schmid, *Adv. Synth. Catal.* **2006**, *348*, 2015–2026.
[17] R. Ruinatscha, K. Buehler, A. Schmid, unpublished results.
[18] A. Schmid, K. Hofstetter, H.-J. Feiten, F. Hollmann, B. Witholt, *Adv. Synth. Catal.* **2001**, *343*, 732–737.
[19] K. Otto, K. Hofstetter, M. Röthlisberger, B. Witholt, A. Schmid, *J. Bacteriol.* **2004**, *186*, 5292–5302.
[20] a) D. Pletcher, F. C. Walsh, *Industrial Electrochemistry*, 2nd edn., Chapman and Hall, London, **1990**; b) H. Wendt, G. Kreysa, *Electrochemical Engineering: Science and Technology in Chemical and Other Industries*, Springer, Berlin, **1999**; c) V. M. Schmidt, *Elektrochemische Verfahrenstechnik: Grundlagen, Reaktionstechnik, Prozessoptimierung*, Wiley-VCH, Weinheim, **2003**.
[21] D. Pletcher, I. Whyte, *J. Appl. Electrochem.* **1991**, *21*, 659–666.
[22] a) L. Gianfreda, M. R. Scarfi, *Mol. Cell. Biochem.* **1991**, *100*, 97–128; b) F. Schulz, F. Leca, F. Hollmann, M. T. Reetz, *Beilstein J. Org. Chem.* **2005**, *1*.
[23] K. H. Dudley, A. Ehrenberg, P. Hemmerich, F. Müller, *Helv. Chim. Acta* **1964**, *47*, 1354–1383.
[24] V. Massey, *J. Biol. Chem.* **1994**, *269*, 22459–22462.
[25] A. M. d. A. Rocha Gonsalves, A. C. Serra, *J. Chem. Soc. Perkin Trans. 2* **2002**, 715–719.
[26] C. Kohlmann, W. Märkle, S. Lütz, *J. Mol. Catal. B: Enzym.* **2008**, *51*, 57–72.
[27] F. Hollmann, K. Hofstetter, A. Schmid, *Trends Biotechnol.* **2006**, *24*, 163–171.
[28] V. L. Vilker, V. Reipa, M. Mayhew, M. J. Holden, *J. Am. Oil Chem. Soc.* **1999**, *76*, 1283–1289.
[29] A. K. Udit, F. H. Arnold, H. B. Gray, *J. Inorg. Biochem.* **2004**, *98*, 1547–1550.
[30] V. Reipa, M. P. Mayhew, V. L. Vilker, *Proc. Natl. Acad. Sci. USA* **1997**, *94*, 13554–13558.
[31] N. Shirane, Z. Sui, J. A. Peterson, P. R. Ortiz de Montellano, *Biochemistry* **1993**, *32*, 13732–13741.
[32] A. Kantz, F. Chin, N. Nallamothu, T. Nguyen, G. T. Gassner, *Arch. Biochem. Biophys.* **2005**, *442*, 102–116.
[33] a) W. A. Duetz, J. B. van Beilen, B. Withold, *Curr. Opin. Biotechnol.* **2001**, *12*, 419–425; b) B. Bühler, A. Schmid, *J. Biotechnol.* **2004**, *113*, 183–210.
[34] J.-B. Park, *Dissertation*, ETH No. 15754, **2004**, Zürich.
[35] S. Panke, M. G. Wubbolts, A. Schmid, B. Witholt, *Biotechnol. Bioeng.* **2000**, *69*, 91–100.
[36] R. J. Beynon, J. S. Easterby, *Buffer Solutions: The Basics*, BIOS Scientific Publishers, Oxford, UK, **1996**.
[37] M. M. Bradford, *Anal. Biochem.* **1976**, *72*, 248–254.
[38] J. D. Genders, D. Pletcher, *Electrosynthesis – from Laboratory to Pilot, to Production*, Electrosynthesis Company, Lancaster, NY, **1990**.
[39] H. Wang, G. A. Capuano, *J. Electrochem. Soc.* **1998**, *145*, 780–784.
[40] J. Wang, *Electrochim. Acta* **1981**, *26*, 1721–1726.
[41] L. G. Whitby, *Biochem. J.* **1953**, *54*, 437–442.

